

# An Adaptive Three-bus Power System Equivalent for Estimating Voltage Stability Margin from Synchronized Phasor Measurements

Fengkai Hu, Kai Sun  
University of Tennessee  
Knoxville, TN, USA  
[fengkaihu@utk.edu](mailto:fengkaihu@utk.edu)  
[kaisun@utk.edu](mailto:kaisun@utk.edu)

Alberto Del Rosso, Evangelos Farantatos,  
Navin Bhatt  
Electric Power Research Institute  
Knoxville, TN, USA  
[adelrosso@epri.com](mailto:adelrosso@epri.com)  
[efarantatos@epri.com](mailto:efarantatos@epri.com)  
[nbhatt@epri.com](mailto:nbhatt@epri.com)

**Abstract**—This paper utilizes an adaptive three-bus power system equivalent for measurement-based voltage stability analysis. With that equivalent identified online, a measurement-based approach is developed to estimate real-time voltage stability margin for a load-rich area supported by remote generation via multiple tie lines. Compared with traditional Thevenin equivalent based approach, this new approach is able to provide more accurate voltage stability margin for each individual tie line. This approach is validated on a three-bus system and the IEEE 39-bus system.

**Index Terms**—parameter estimation; phasor measurement unit; Thevenin equivalent; voltage stability monitoring

## I. INTRODUCTION

Voltage instability is a major concern for power systems operation. Usually, it initiates from a local bus or region but may develop to a wide-area or even system-wide stability problems. Online Voltage Stability Assessment (VSA) is a key function in system operations to help operators foresee potential voltage insecurity. Traditional VSA is based on a simulation-based approach. By either power-flow analysis or time-domain simulation, it employs power system models to simulate a list of contingencies on a State Estimator solution that represents the current operating condition. However, the simulation based approach has limitations: it is model-dependent and it requires a convergent State Estimation solution for the current operating condition.

Different measurement-based VSA approaches have been studied to directly estimate real-time voltage stability margin for a monitored load bus or area [1]-[9] or predict potential post-contingency voltage insecurity by means of data mining techniques [10]. A majority of the measurement-based approaches are based on Thevenin's Theorem. For instance, local measurements at the monitored buses are used to approximate the rest of the system as an impedance connected

to a voltage source, i.e. the Thevenin equivalent. The power transferred to the bus reaches its voltage stability limit when that external Thevenin impedance has the same magnitude as the load impedance at the bus [1]. Based on Thevenin equivalent, the voltage stability or reactive-power reserve indices can be obtained [2]-[5]. A modified model with two equivalent voltage sources is studied in [6] to predict the stability limit. Paper [7] applies the Thevenin equivalent based approach to an actual EHV network. Some other works consider load tap changers and over-excitation limiters in their models for better detection of voltage instability [8][9]. The above methods work well on a radially-fed load bus or transmission corridors. EPRI developed a Thevenin equivalent-based method for load center areas, which requires synchronized measurements on boundary buses [4][5]. As illustrated by Fig. 1, the method merges all boundary buses and tie lines to one fictitious boundary bus connected by one tie line with the external system such that the Thevenin equivalent can be applied. An ongoing project is demonstrating this method in the real-time environment [11].

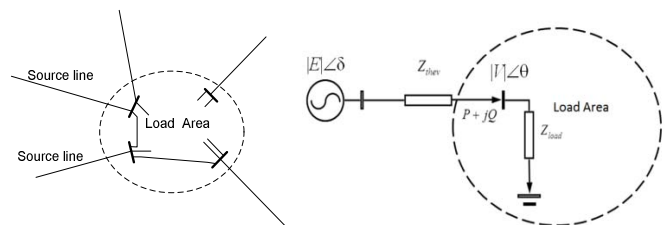


Figure 1. Load area and its Thevenin equivalent

However, the Thevenin equivalent-based approach cannot provide voltage stability margin for each individual tie line when the monitored load is fed by multiple tie lines. For such a case, transfer limits of various tie lines may be reached at different times, or in other words, voltage instability may start near one of the boundary buses sooner and then progress to

the others. However, by monitoring the total transfer limit through a single equivalent, the Thevenin equivalent based approach may not detect the time variability across the interface associated with voltage instability.

In this paper, an adaptive three-bus power network equivalent is proposed for estimating voltage stability margin for a load-rich area fed by multiple tie lines. A real-time voltage stability monitoring method is then developed based on that new equivalent. It is explained and demonstrated later that such a three-bus equivalent, if applied to a load-rich area fed by two or more tie lines, is able to estimate the real-time power transfer limit in terms of voltage stability for each individual tie line if synchronized measurements are available on all boundary buses. This new method is tested on a three-bus system and the IEEE 39-bus system.

## II. A THREE-BUS EQUIVALENT

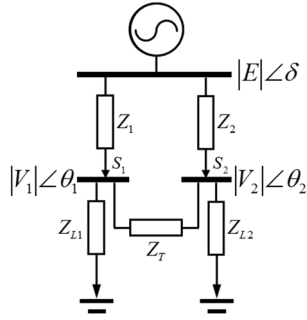


Figure 2. Proposed 3-bus equivalent

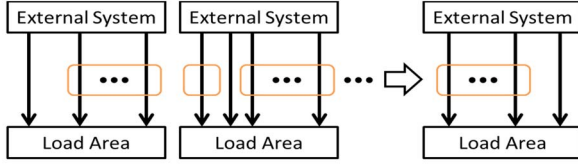


Figure 3. Strategies for three-bus equivalencing –  $N$  equivalents

As shown in Fig. 2, a three-bus power network equivalent is proposed to monitor voltage stability for a load-rich area. Its three buses include a voltage source and two interconnected load buses representing the load center. The voltage source represents the external system, whose generators are assumed to be strongly coherent without risking any angular instability. The two load buses represent either actual or fictitious boundary buses, depending on the requirement of voltage stability monitoring. For example, if it is required to estimate the transfer limit for each of the  $N$  tie lines of a load area, any tie line versus the rest can be studied to create  $N$  three-bus equivalents, as illustrated by Fig. 3. Then, voltage stability analyses on all such equivalents provide comprehensive results on all tie lines. In practice, usually only one or very few tie lines are most vulnerable to voltage instability, so it is unnecessary to study all  $N$  equivalents. Since this equivalent does not model generator VAR limit, it focuses on detecting or predicting the saddle-point bifurcation type voltage collapse on the load side [12]. However, since the equivalent will be estimated in real time from measurement data, it also has

potentials in reflecting significant changes on the generation side, e.g. voltage drops due to a generator limit being met.

## III. APPROACH FOR VOLTAGE STABILITY MARGIN CALCULATION

Based on the three-bus equivalent, an approach for calculating voltage stability limits and margins for  $N$  tie lines of a load area is presented in this section. The approach assumes that time-synchronized voltage phasor data  $\bar{V}_1 \sim \bar{V}_N$  at boundary buses and current phasor data  $\bar{I}_1 \sim \bar{I}_N$  of tie lines are available. The data may be from synchrophasors, e.g. phasor measurement units (PMUs) at 30-60 samples per second or a state estimator at a slower rate, e.g. 20s to several minutes, depending on the speed requirements for voltage stability monitoring. This paper uses synchrophasor data as an example. The approach conducts the following steps:

- i) Determine the number of three-bus equivalents, depending on how many lines need to be monitored in detail for power transfer limits and margins. For each equivalent, use measurements to calculate voltage phasor data of  $V_1$  and  $V_2$  and complex power-flow data of  $S_1$  and  $S_2$  on two load buses as indicated by Fig. 2. For instance, if the 1<sup>st</sup> bus is selected vs. the others,  $V_1$ ,  $V_2$ ,  $S_1$  and  $S_2$  are calculated by (1)

$$\begin{aligned} V_1 &= \bar{V}_1, & S_1 &= \bar{V}_1 \bar{I}_1^* \\ V_2 &= \sum_{i=2}^N \bar{V}_i \bar{I}_i^* / \sum_{i=2}^N \bar{I}_i^*, & S_2 &= \sum_{i=2}^N \bar{V}_i \bar{I}_i^* \end{aligned} \quad (1)$$

- ii) At any time when estimation of stability limits or margins is expected, use the data of  $V_1$ ,  $V_2$ ,  $S_1$  and  $S_2$  over a latest time window to estimate the other parameters of the three-bus equivalent including those of the external system, i.e.  $E$ ,  $Z_1$ ,  $Z_2$ , and those of the load area, i.e.  $Z_{L1}$ ,  $Z_{L2}$  and  $Z_r$ . Details are presented in subsections A and B.
- iii) Find the maximum limit of the active power transferred to each of the two load buses, denoted by  $P_{1\max}$  and  $P_{2\max}$ . An exhaustive or heuristic searching algorithm may be employed to find the limit. Since the searching space is not large for the three-bus equivalent, subsection C gives an algorithm for exhaustive searching.

### A. External System Parameters Estimation

Assume that  $E$ ,  $Z_1$  are  $Z_2$  are constant over the time window. Thus, similar to [1], a least-square method may be adopted to give estimates for  $E$ ,  $Z_1$  are  $Z_2$ . Note that the Thevenin equivalent has 4 real unknowns while this new equivalent has 6 real unknowns to solve, i.e.:

$$[E_r \ E_i \ R_1 \ X_1 \ R_2 \ X_2] = (H^T H)^{-1} H^T Z \quad (2)$$

where  $E_r + jE_i = E$ ,  $R_1 + jX_1 = Z_1$ ,  $R_2 + jX_2 = Z_2$ , and matrices  $H$  and  $Z$  are formed based on measurement data at  $n$  time points of the time window.  $V_{1r,k}$  and  $V_{1i,k}$  respectively denote the real and imaginary parts of bus 1 voltage at the  $k$ -th time point.  $p_{1,k}$  and  $q_{1,k}$  are respectively the active and reactive powers received by bus 1 at the  $k$ -th time point. Similarly,  $V_{2r,k}$ ,  $V_{2i,k}$ ,  $p_{2,k}$  and  $q_{2,k}$  are data of bus 2.

$$H = \begin{bmatrix} V_{1r,1} & V_{1i,1} & -p_{1,1} & -q_{1,1} & 0 & 0 \\ V_{1i,1} & -V_{1r,1} & -q_{1,1} & p_{1,1} & 0 & 0 \\ V_{2r,1} & V_{2i,1} & 0 & 0 & -p_{2,1} & -q_{2,1} \\ V_{2i,1} & -V_{2r,1} & 0 & 0 & -q_{2,1} & p_{2,1} \\ \vdots & \vdots & \vdots & \vdots & \vdots & \vdots \\ V_{1r,n} & V_{1i,n} & -p_{1,n} & -q_{1,n} & 0 & 0 \\ V_{1i,n} & -V_{1r,n} & -q_{1,n} & p_{1,n} & 0 & 0 \\ V_{2r,n} & V_{2i,n} & 0 & 0 & -p_{2,n} & -q_{2,n} \\ V_{2i,n} & -V_{2r,n} & 0 & 0 & -q_{2,n} & p_{2,n} \end{bmatrix} \quad (3)$$

$$Z^T = [V_{1r,1}^2 + V_{1i,1}^2 \quad 0 \quad V_{2r,1}^2 + V_{2i,1}^2 \quad 0 \quad \dots \quad V_{1r,n}^2 + V_{1i,n}^2 \quad 0 \quad V_{2r,n}^2 + V_{2i,n}^2 \quad 0] \quad (4)$$

### B. Load Area Parameters Estimation

To estimate the load area parameters, at least two time points (denoted by  $t_a$  and  $t_b$ ) of measurement data are needed. The following equations could be obtained:

$$\begin{aligned} |V_{1a}|^2 Y_{11a} + (|V_{1a}|^2 - V_{1a}^* V_{2a}) Y_{12} &= S_{1a}^* \\ |V_{1b}|^2 Y_{11b} + (|V_{1b}|^2 - V_{1b}^* V_{2b}) Y_{12} &= S_{1b}^* \\ |V_{2a}|^2 Y_{22a} + (|V_{2a}|^2 - V_{2a}^* V_{1a}) Y_{12} &= S_{2a}^* \\ |V_{2b}|^2 Y_{22b} + (|V_{2b}|^2 - V_{2b}^* V_{1b}) Y_{12} &= S_{2b}^* \end{aligned} \quad (5)$$

Symbols labelled ‘‘a’’ or ‘‘b’’ are linked to the corresponding time  $t_a$  or  $t_b$ . For example,  $V_{1a}$  denotes the bus 1 voltage phasor at time  $t_a$ .  $Y_{11a}$  denotes the admittance of the load connected to bus 1.  $Y_{12}$  represents the transfer admittance between the two load buses, which is assumed constant. Another assumption is that each load impedance has a constant impedance angle, i.e. constant power factor. Thus,

$$G_{11a} / B_{11a} = G_{11b} / B_{11b}, \quad G_{22a} / B_{22a} = G_{22b} / B_{22b} \quad (6)$$

Equations (5) and (6) actually correspond to 10 real equations, which are solved for 10 real unknowns, i.e. real and imaginary parts of complex unknowns  $Y_{12}$ ,  $Y_{11a}$ ,  $Y_{11b}$ ,  $Y_{22a}$  and  $Y_{22b}$ . The above constant power factor assumption can tolerate reasonably slight changes in the impedance angles over a short time window based on our studies.

### C. Finding the Power Transfer Limits

Based on the current operating condition, which depends on the estimated  $Z_{L1}$  and  $Z_{L2}$ , the maximum limits of the active power transferred to two load buses need to be solved. It is assumed that  $Z_{L1}$  and  $Z_{L2}$  vary in a zone and then an exhaustive search is conducted to check power-flow solutions of all meshed representative points in that space. The goal is to find the maximum power flows delivered to the two load buses without causing voltage insecurity.

Since the dimension of the space is not high, those points may have a very high density. Also, when solving the power-flow solution at each point, the power injected by the slack bus is limited within a range around its original value to avoid unrealistically large changes at the slack bus. A heuristic algorithm may also be applied to utilize the gradient information from two successive points during the searching to speed on the process.

## IV. CASE STUDIES

A three-bus system and the IEEE 39-bus system are used to test the proposed approach. Simulations are conducted and the simulation results at the boundary buses are treated as synchrophasor data.

### A. Three-bus System

The three-bus system has the same structure as the equivalent shown in Fig. 2 with all parameters given below in per unit:

$$\begin{aligned} E &= 1.0475 \angle 0, Z_1 = 0.002 + j0.02, Z_2 = 0.03 + j0.1, \\ Z_{L1} &= 1.9953 + j0.5915, Z_{L2} = 1.2746 + j0.3405 \end{aligned}$$

Time-domain simulations are conducted to continuously decrease the magnitudes of two load impedances by 1% every second to simulate a load area with increasing load until two lines meet the maximum power transfer limits. The purposes of this case are to demonstrate: 1) how different the limits of two lines may be, and 2) differences between the results of this new approach and those from a traditional Thevenin equivalent based approach.

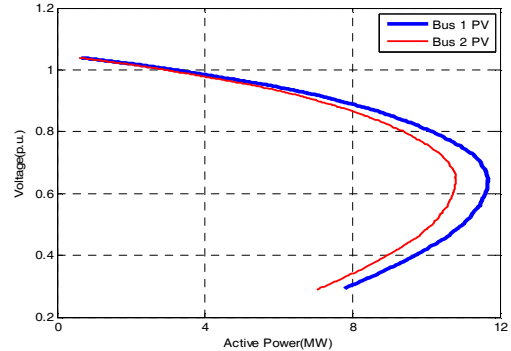


Figure 4. PV curves of two load buses with tight interconnection

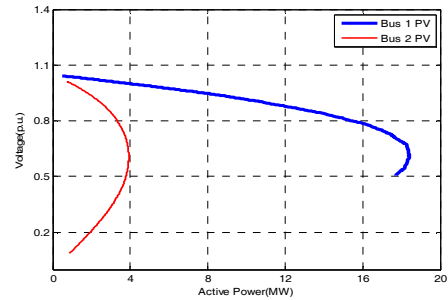


Figure 5. PV curves of two load buses with weak interconnection

Two cases are simulated with two different values of the transfer impedance  $Z_{12}$ , i.e.  $0.00003 + j0.0005$  pu and  $0.03 + j0.5$  pu, which respectively represent a tight interconnection and a relatively weak interconnection between the two load buses (corresponding to the boundary buses of the load area). Fig. 4 and Fig. 5 give the PV curves from simulation results at two load buses. Each curve is about the bus voltage magnitude and the active power transferred to the bus. When the two load buses are more weakly connected, the

two P-V curves are more different, indicating the need of the estimating stability limits for individual buses.

The proposed approach is performed every 1 second over a sliding time window of 1 second. For tight and weak interconnections, Fig. 6 gives the active line flows  $P_1$  and  $P_2$ , and total interface flow  $P_1+P_2$ , and their limits calculated by the new approach, i.e.  $P_{1max}$ ,  $P_{2max}$ , and  $P_{max(new)} = P_{1max}+P_{2max}$ . For comparison purposes, the total interface flow from the Thevenin equivalent based approach is also given as  $P_{max(Thevenin)}$  in the figures. Based on the results, it can be observed that when the two interface buses have tighter interconnection, the transfer limits of the two lines are met at the same time [around  $t=380s$  in Fig. 6(a)], which means the two buses can be reasonably merged into one bus without losing accuracy. That is the basic assumption of the traditional Thevenin equivalent based approach, so the Thevenin equivalent based approach also estimates the total interface limit to be met almost at the same time as individual lines. As shown by Fig. 6(b), when the two buses are weakly connected, the limits of two lines are met at different time instants, at  $t=470s$  and  $t=260s$ , respectively. On the other hand, the Thevenin equivalent based approach estimates that the total interface flow limit is met at around  $t=370s$ , i.e. not much different from the tight interconnection case. The results illustrate that if only the total transfer limit for the entire interface of a load area is estimated, detection of voltage instability may be delayed since some tie line may be more stressed and voltage instability may occur there first.

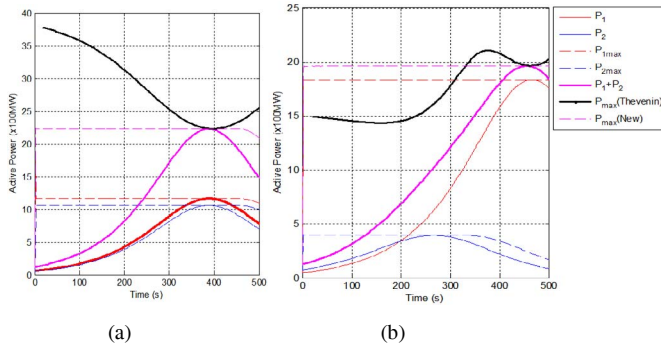


Figure 6. Line flow limits for tight (a) and weak (b) interconnections between two buses

## B. IEEE 39-bus System

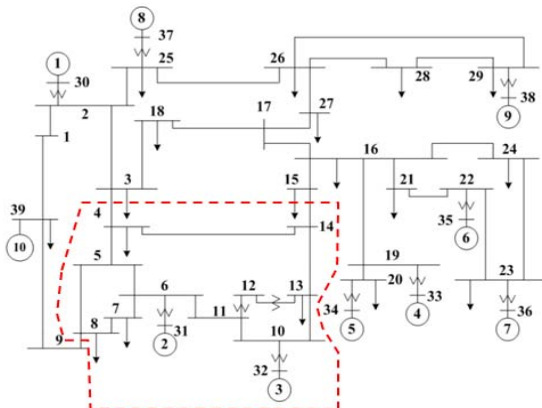


Figure 7. IEEE 39-bus system diagram

For the IEEE 39-bus system, a load area is defined as indicated by Fig. 7. It has three interface buses, i.e. buses 4, 8 and 14. The system can be simplified into a three-bus equivalent system, and utilize the approach proposed in this paper. The following contingency is simulated to create a voltage instability scenario:

- Starting from  $t=0s$ , keep increasing the total load of the area from 1898 MW at a speed around 1.3MW (with slight randomization) per second to create slow decay in the voltage level of the area.
- At  $t=439s$ , trip the generator on bus 32, i.e. one of the two local generators of the load area.
- Keep increasing the load of the area at the same speed until voltage collapse around  $t=539s$ .

Fig. 8 shows all bus voltage magnitudes, in which the highlighted curves are those inside the load area.

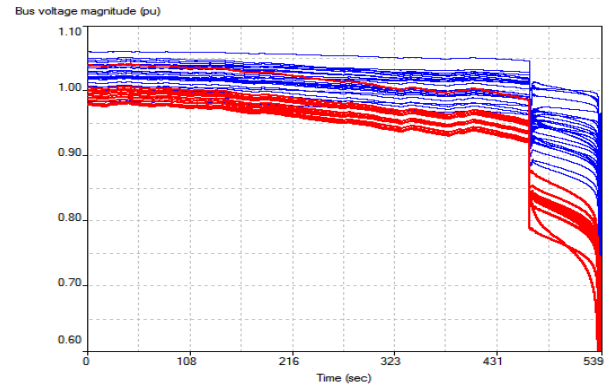


Figure 8. New England system bus voltage magnitude

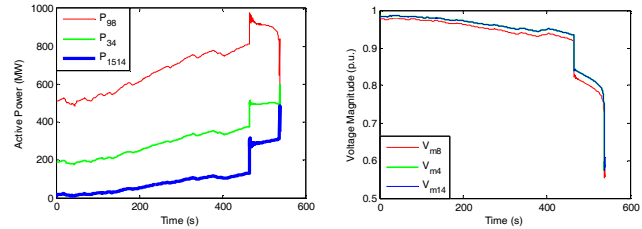


Figure 9. Active power and voltage magnitude of buses on the boundary

Fig. 9 gives the active power flows and the bus voltage magnitudes of three boundary buses. Bus 4 and bus 14 have close voltage curves, so they can be merged into a single fictitious bus, named bus E. The two lines connected, i.e. 15-14 and 3-4, are also merged to an equivalent line, named line E. Thus, the three-bus equivalent is applied. Fig. 10 gives the active power flows of line 9-8 and line E and the voltage magnitudes at bus 8 and bus E. Fig. 11 gives the P-V curves from the simulation results on the two buses. It shows that two curves have different shapes and their “nose” points may be reached at different times in the simulation.

Parameters of the external system and load area are estimated at each time step of 0.25s using measurements (i.e. from simulation results) on the three boundary buses over the latest 5s time window. Let  $P_{98}$  and  $P_E$  denote the active powers

in the line 9-8 and line E, whose real-time values are directly from the measurements. At each time step, in the plane about  $P_{98}$  and  $P_E$ , a rectangular region of  $\pm 50\%$  around the point corresponding to their real-time values is considered. Power flow solutions are studied for representative points in the region at a density. The real power change at the slack bus for each time step is restricted to 20% in solving the power flows. The maxima of  $P_{98}$  and  $P_E$ , i.e.  $P_{98max}$  and  $P_{Emax}$ , among all solved power flows are identified as the limits of the two lines in terms of voltage stability. Fig. 12 gives the identified active power limits. Fig. 13 compares the percentage active power margins, i.e.  $(P_{98max}-P_{98})/P_{98}\times 100\%$  and  $(P_{Emax}-P_E)/P_E\times 100\%$ . At the beginning, the percentage margin of  $P_{98}$  is larger than that of line E. Two margins become closer after the generator trip at  $t=439s$ . Finally, the voltages at two buses almost collapse at the same time. The generator trip has more impact on the voltage stability margin of line E because the tripped generator is closed to bus 4 and bus 14. Such information is not available from a traditional Thevenin equivalent based approach. This new approach offers more accurate monitoring of voltage stability margins for individual tie lines.

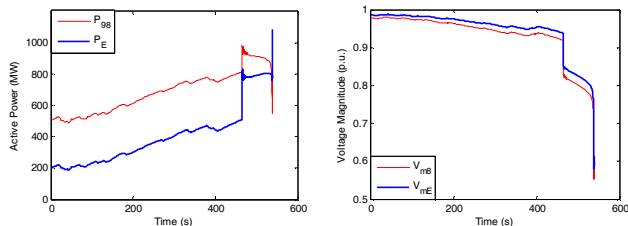


Figure 10. Bus equivalent result

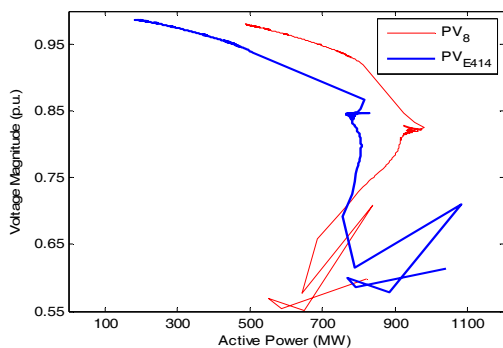


Figure 11. PV curves of two buses in England New system

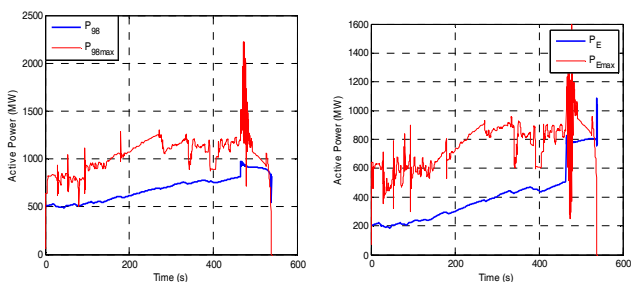


Figure 12. Active powers of two lines and their voltage stability limits

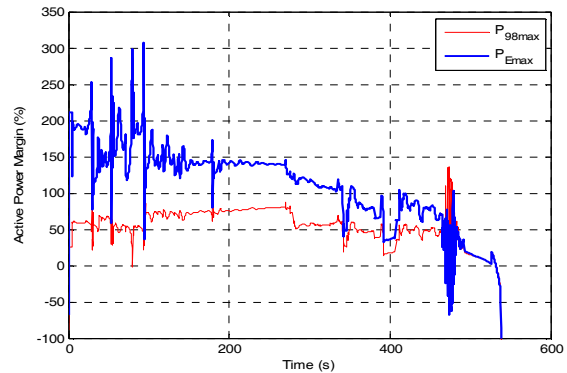


Figure 13. Comparison of the percentage active power margins of two lines

## V. CONCLUSION

This paper proposed a new three-bus equivalent for real-time estimation of voltage stability margin using synchronized measurements at the boundary buses of a load area. The detailed approach was compared to the traditional Thevenin equivalent based approach by case studies. The comparison indicates that the new approach is able to assess voltage stability limits of a load area served by multiple lines more accurately than the traditional approach.

## VI. REFERENCES

- [1] K. Vu, M. Begovic, D. Novosel, and M. Saha, "Use of local measurements to estimate voltage-stability margin," *IEEE Trans. Power Systems*, vol. 14, no. 3, pp. 1029–1035, Aug. 1999.
- [2] B. Milosevic and M. Begovic, "Voltage-stability protection and control using a wide-area network of phasor measurements," *IEEE Trans. Power Systems*, vol. 18, pp. 121–127, 2003.
- [3] Smon, et al, "Local Voltage-Stability Index Using Tellegen's Theorem," *IEEE Trans. Power Systems*, Vol. 21, No. 3, Aug. 2006.
- [4] P. Zhang, L. Min, et al, "Measurement based voltage stability monitoring and control", US Patent # 8,126,667, Feb 2012.
- [5] K. Sun, P. Zhang, L. Min, "Measurement-based Voltage Stability Monitoring and Control for Load Centers", EPRI Technical Report No. 1017798, 2009.
- [6] M. Parniani, et al, "Voltage Stability Analysis of a Multiple-Infed Load Center Using Phasor Measurement Data," *IEEE PES Power Systems Conference and Exposition*, Nov 2006
- [7] S. Corsi and G. Taranto, "A real-time voltage instability identification algorithm based on local phasor measurements," *IEEE Trans. Power Systems*. vol. 23, no. 3, pp. 1271–1279, Aug. 2008.
- [8] C. D. Vournas and N. G. Sakellaridis, "Tracking Maximum Loadability Conditions in Power Systems," in 2007 *iREP Symposium Bulk Power System Dynamics and Control - VII. Revitalizing Operational Reliability*, 2007.
- [9] M. Glavic and T. Van Cutsem, "Wide-Area Detection of Voltage Instability from Synchronized Phasor Measurements. Part I: Principle," *IEEE Trans. Power Systems*, vol. 24, pp. 1408 - 1416, 2009.
- [10] R. Diao, K. Sun, V. Vittal, et al, "Decision Tree-Based Online Voltage Security Assessment Using PMU Measurements", *IEEE Trans. Power Systems*, vol. 24, pp.832-839, May 2009.
- [11] F. Galvan, A. Abur, K. Sun, et al, "Implementation of Synchrophasor Monitoring at Entergy: Tools, Training and Tribulations", *IEEE PES General Meeting*, 23-26 July 2012, San Diego
- [12] C. Canizares, et al, *Voltage Stability Assessment: Concepts, Practices and Tools*, IEEE PES Power System Stability Subcommittee Special Publication, IEEE, Aug 2002